ELSEVIER

Ceramics International 26 (2000) 123–132

CERAMICS INTERNATIONAL

Tin dioxide thin film gas sensor

A.K. Mukhopadhyay*, P. Mitra, A.P. Chatterjee, H.S. Maiti

Composite Division, Central Glass and Ceramic Research Institute, Calcutta 700 032, India

Received 19 January 1999; received in revised form 21 February 1999; accepted 21 April 1999

Abstract

Tin dioxide (SnO_2) is the singular, most important material utilised in commercially manufactured sensors for toxic and combustible gases. In the present work, tin dioxide thin film sensors with porous microstructure and thickness of 0.22 μm have been fabricated on commercially available glass slides by a novel, low-cost, modified chemical deposition technique. Here we report, for the first time, the details of structural and deposition characteristics of the same films as a function of experimental parameters such as the number of dippings, bath temperature and bath concentration. In addition, the electrical properties were studied for both as deposited and palladium sensitised films as a function of temperature (300–500 K) in a closed quartz tube furnace. Further, the gas sensitivity of the palladium sensitised tin dioxide thin film sensors was evaluated in air inside the same closed quartz tube furnace as a function of the operating temperature (150–300°C) for a fixed concentration (3 vol%) of hydrogen gas with nitrogen as the carrier gas. The sensor response could be recorded at an operating temperature of as low as 150°C. Maximum sensitivity of 90% was found to occur at a low temperature of only 200°C. Above this cut-off temperarure, sensitivity of the present thin film sensors was found to suffer only moderate degradation.

Keywords: SnO_2; Thin film; Gas sensor

1. Introduction

Tin dioxide (SnO_2), the most important material for commercially manufactured gas sensors, is an *n*-type semiconductor with a relatively wide band gap energy (E_g) of 3.5 eV. The intrinsic conduction mechanism of SnO_2 is usually linked to bulk oxygen vacancies [1–4]. A considerable amount of current research activities has been devoted to the development of stable, pure or doped tin dioxide sensors [1–9]. These sensors are developed mostly as thin films [1–15], and occasionally as thick films/bulk pellets [16–18], presumably, due to the higher sensitivity of the former. SnO_2 thin films have been prepared by a variety of techniques such as sputtering, ion-assisted reactive evaporation, chemical vapour deposition, metal organic chemical vapour deposition, spray pyrolysis, dip coating, sol-gel, chemical deposition etc. [2–15]. Of these, the chemical deposition offers the lowest cost of production, easier control over film thickness and a porous microstructure essential for promotion of surface chemisorption that induces gas sensing. A minimum operating temperature of about 200–400°C is commonly observed for SnO_2 sensors exposed to toxic and combustible gases [5–7].

We have recently reported the fabrications of both zinc oxide (ZnO) and tin dioxide thin film gas sensors by novel, modified chemical deposition techniques [19–22]. These sensors were found to have high sensitivity at operating temperatures of as low as 150°C.

Here we report, for the first time, the details of structural and deposition characteristics as a function of experimental parameters as well as electrical and gas sensitivity properties as a function of the operating temperature for a fixed value (3 vol%) of hydrogen gas concentration, for these SnO_2 thin films synthesised by the novel, low-cost, modified chemical deposition technique [19].

2. Experimental

The tin dioxide thin films were deposited on precleaned substrates. Commercially available microscope glass slides of 2.1 mm thickness were used as substrates.

* Corresponding author. Tel.: +91-33-473-3469; fax: +91-33-473-0957.

E-mail address: anoop@cscgcri.ren.nic.in (A.K. Mukhopadhyay).

0272-8842/00/$20.00
PII: S0272-8842(99)00029-2

The sequence of substrate cleaning steps was: 2 min rinse in each of distilled water, double distilled water and deionised water followed by 2 min of ultrasonic cleaning in a equivolume mixture of acetone and ethyl alcohol. The cleaned substrate was tightly held in a holder so that an effective area of 40×30 mm was exposed. Next, the substrate was successively dipped in a sodium sulphide (Na_2S) bath (0.025 M) kept at room temperature and a stannous chloride ($SnCl_2$) bath (0.025 M) kept at 85°C. This sequence was repeated for the requisite number of times to induce growth of tin sulphide (SnS) film. This SnS film was subsequently oxidised for 1 h. at 400°C in air to obtain the porous, thin films of SnO_2 [19].

Film thickness was measured gravimetrically, following Refs. [19–22]. Theoretical density of SnO_2 was assumed as 6.95 gm cc^{-1} [23]. The deposition rate process data were obtained by varying the film thickness as a function of the number of dips, [$N = 25-300$], temperature of $SnCl_2$ bath (70–100°C) and concentration of both Na_2S and $SnCl_2$ baths (0.025–0.2 M).

Phase purity of the deposited films was examined by the X-ray diffraction (XRD) technique using a Ni filter and Cu-Kα radiation. Scanning electron microscopy (SEM) was used to reveal the microstructure of the deposited films. To prepare samples for studying by the SEM technique, SnO_2 films were deposited on smaller substrates (5×5×2 mm). To avoid charging effects, a 100 Å thin layer of gold was evaporated on top of the SnO_2 films, prior to insertion in the SEM chamber. All SEM photographs were taken with a secondary electron detector.

The conductance versus temperature data of SnO_2 thin films (40×30 mm) were obtained in a closed quartz tube furnace in air using the conventional two probe method with Ag contacts (dia∼1 mm, length ∼20 mm, separation ∼3 mm) following [19–22]. The range of temperature investigated was 300–500 K with a control accuracy of (±) 1 K. The data on conductance vs temperature were obtained for unsensitised, i.e. as deposited films, as well as for film surfaces sensitised with Pd using a novel, wet chemical technique [20]. Thermal cycling experiments were also conducted on the same films on several consecutive days to examine the possibilities of resistance stabilisation. The data on temperature dependence of conductance (Σ) were analysed using the equation:

$$\Sigma = \Sigma_o \exp(-E_b/kT) \quad (1)$$

where, Σ_o is the pre-exponential term, E_b is the activation energy, k is the Boltzmann's constant and T is the test temperature in absolute scale.

The gas sensitivity studies of the Pd-sensitised SnO_2 thin film was conducted in the same closed quartz tube furnace as mentioned above [19]. Sensitivity was found out in air as a function of operating temperature (150–300°C) for a fixed concentration (3 vol%) of hydrogen (H_2) gas with nitrogen as carrier gas (N_2). At each operating temperature, the sensor was allowed to equilibriate for 15 min prior to gas exposure. In each occasion, following a 30 min exposure the gas flow was turned off. Then, the sensor was allowed to recover in air.

The sensitivity (S) was measured in terms of the percentage reduction in the sensor resistance ratio with time as:

$$S = \left[\left\{R_g/R_a\right\} \times 100\right] \quad (2)$$

following Refs. [19–22]. Here, R_a is the sensor resistance in air (prior to gas exposure) and R_g is the sensor resistance in presence of the target gas.

3. Results and discussion

3.1. Deposition process

The data on the deposition process of the SnO_2 thin films as a function of the experimental parameters are shown in Fig. 1(a)–(d). Error bars in this figure represent typical overall average scatter in the data. Up to 50 dips, the deposition process was fairly linear, with a rate of 0.28 μm/dip/mol [Fig. 1(a)]. At a higher number of dips ($N = 50-300$), the growth of film thickness followed a distinctly non-linear trend [Fig. 1(b)]. Subsequent experiments to get data on the deposition process as functions of $SnCl_2$ bath temperature and concentration were, therefore, limited to 50 dips only, [Fig. 1(c) and (d)]. $SnCl_2$ bath temperatures below ∼85°C do not seem to have any significant influence on film thickness (t), [Fig. 1(c)]. At temperature >85°C, film thickness increased with bath temperature.

Film thickness (t) increased non-linearly with enhancement in $SnCl_2$ bath concentration (C), [Fig. 1(d)]. The data, however, show two different slopes indicating that different reaction rates may be involved at concentrations, C less than 0.1 M and greater than 0.1 M.

To explain these observations we resort back to the initial chemical processes that occur in situ on the substrate. Primarily the following reaction:

$$SnCl_2 + Na_2S = 2NaCl + SnS \quad (3)$$

took place most likely on the substrate. This induced isolated nuclei formation. As the sequence was repeated for the requisite number of times; isolated nuclei formation, followed by localised build-up, collapse and growth of adherent SnS film were affected on the glass substrate. When this thin SnS layer was oxidised, the following reaction happened:

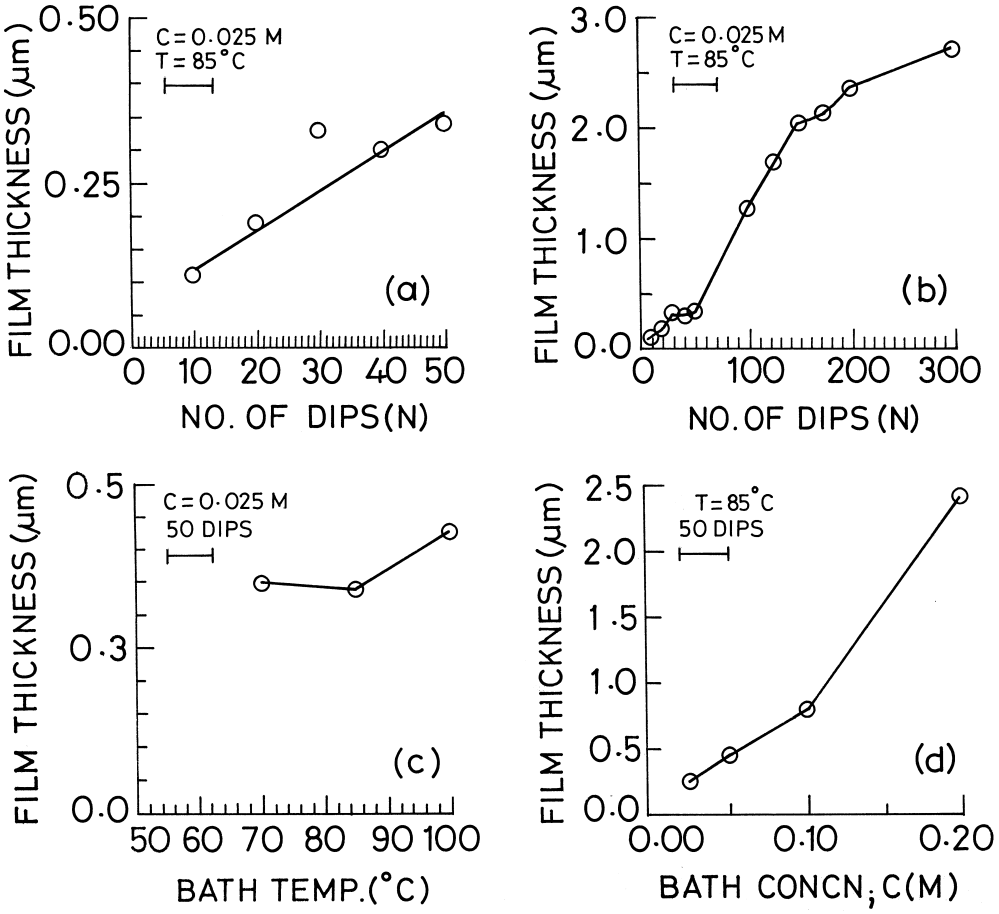

Fig. 1. Variation of SnO_2 film thickess with (a) a smaller number of dips ($N = 0-50$), (b) a larger number of dips ($N = 0-300$), (c) temperature of $SnCl_2$ bath at fixed concentration ($C = 0.025$ M) and number of dips ($N = 50$) and (d) concentration of $SnCl_2$ bath at fixed bath temperature (85°C) and number of dips ($N = 50$).

$$SnS + O_2 = SnO_2 + SO_2 \quad (4)$$

This led to the formation of porous SnO_2 thin films with a matty white appearence [19].

The initial linear trend in film thickness with the number of dips may imply two aspects: (a) up to N less than or equal to 50, the rates of forward and backward reactions at the substrate solution interface in formation of SnS thin film were equally slow and constant; and (b) there was almost complete conversion of SnS thin film to SnO_2. This second suggestion is supported by XRD data (Fig. 2). Thus, on completion of the entire dipping process each time, the same amount of reactants were involved in producing the same constant amount of SnS which was subsequently converted to SnO_2, as long as the total number of dips (N) was restricted to less than or equal to 50 [Fig. 2(a)].

As the number of dips was increased, the trend in film thickness versus number of dips became non-linear. This might indicate the possibilities: (a) at film thickness, t, greater than 0.35 μm, the rates of forward and backward reactions in Eq. (3) became unequal; and (b) since oxidation follows parabolic kinetics generally, the conversion of SnS to SnO_2 becomes more complete in thinner films (e.g. $N = 50$) than in thicker films (e.g. $N = 100$) [Fig. 2(b)]. All oxidation runs were done for 1 h. only in air at 400°C, irrespective of film thickness.

The data of Fig. 1(a) and (b) also imply that the overall reaction process was very slow and indeed this led to formation of quite thin SnO_2 films. Increase in $SnCl_2$ bath temperature was done to have a faster deposition rate. However, this did not have an appreciable effect on the reaction process and so, the variation in film thickness was not affected to a significant degree [Fig. 1(c)]. The data of Fig. 1(d) are plotted as a function of the $SnCl_2$ bath concentration (C). It must be mentioned that the corresponding Na_2S baths had concentrations equal to those of the $SnCl_2$ baths. At the fixed temperature (85°C) of the $SnCl_2$ bath, the present data indicated different growth rates, e.g. 0.16 μm/dip/mol for C less than or equal to 0.1 M and 0.34 μm/dip/mol for any value of C in the range of 0.1–0.2 M. The reason for this is yet to be clearly understood. However, enhanced bath concentrations should imply that at the beginning of each dipping process, higher amount of reactants were present at the substrate–solution interface.

This may affect the rate of nucleation and hence, film growth at concentrations below and above the critical one, i.e. $C = 0.1$ M.

3.2. Phase and microstructure

As mentioned earlier, Fig. 2(a) and (b) shows the XRD spectra for SnO_2 thin films deposited by 25 dips and 100 dips, respectively. Up to 50 dips the phase purity of the present SnO_2 films is evidently preserved. In these films, the (110) plane has the highest intensity, as expected for a casseterite crystal structure. Other major planes are (101), (200) and (211) [Fig. 2(a)]. However, as the films grew thicker e.g. $N = 100$, the Sn_2O_3 phase appeared along with SnO_2 phase [Fig. 2(b)]. XRD data for still thicker films (e.g. $N = 300$), not shown here, exhibited features similar to those shown in Fig. 2(b). Similarly, XRD data obtained corresponding to Fig. 1(c), but not shown here, exhibited the fact that at film thicknesses higher than 0.4 μm, small amounts of minor phases were present in a way similar to that shown in Fig. 2(b). Based on the data of deposition rate process and the XRD investigations; all the subsequent studies were done on films of thickness 0.22 (±) 0.04 μm obtained after 25 dips; so that all data correlates to phase pure SnO_2 films deposited at 85°C temperature of $SnCl_2$ bath and with 0.025 M concentrations of both the Na_2S and the $SnCl_2$ baths.

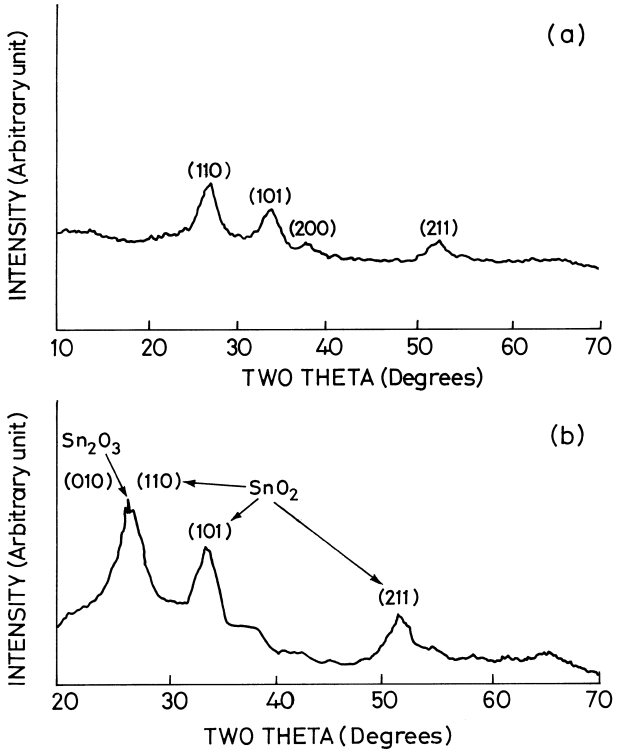

Fig. 2. XRD spectra of SnO_2 thin film deposited with (a) 25 dips and (b) 100 dips.

The microstructure of SnO_2 thin films deposited after 25 and 100 dips are shown in Fig. 3(a) and (b). These SEM photographs indicate that both the films had a porous microstructure with very fine pores distributed nearly uniformly on the film surface. In addition, both the films had crystallite size in the range of few tens to a few hundreds of angstroms (Å) only. The spatial density of these very fine sized crystallites appear to be more in the thicker film than in the thinner film [Fig. 3(a)]. Thus, the thinner film was more porous than the thicker film. The present observation also imply that size of crystallites was even smaller in the thicker film than in the thinner film. This can be explained as follows. With higher number of dippings, more nuclei are formed on the substrate. Thus, the reactant atoms arriving at the substrate-solution interface would diffuse onto the substrate surface and eventually, reach the nuclei which are already growing. As the spatial density of these nuclei becomes significantly large, the size of crystallites are constrained to be very small because, the effective area of depositon for all the films is constant.

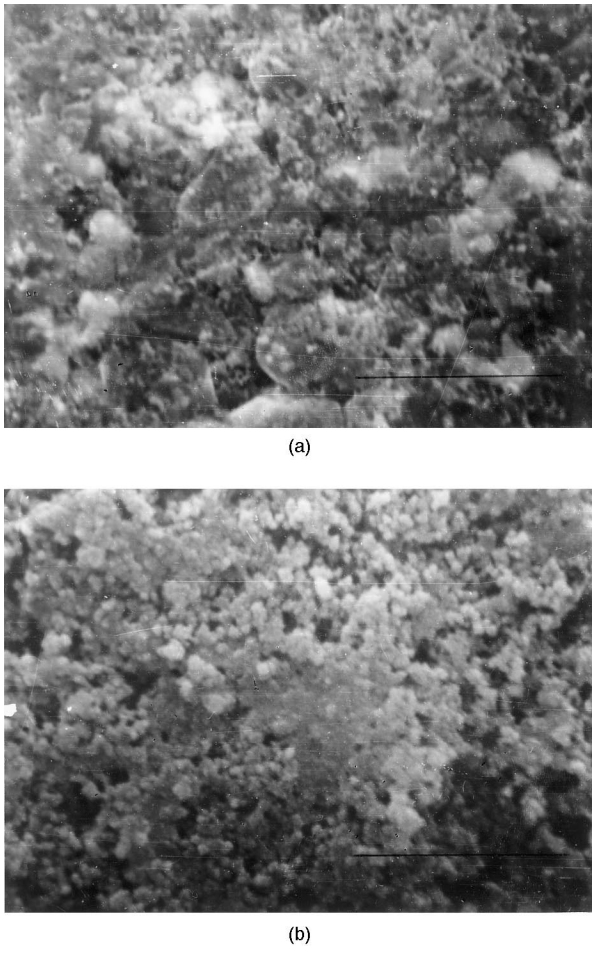

Fig. 3. Scanning electron micrograph of SnO_2 thin film deposited with (a) 25 dips (scale bar = 4 μm) and (b) 100 dips (scale bar = 2 μm). Notice that crystallite size ranges from a few tens to a few hundreds of Å.

The crystallite size was reported to have significant effect on sensitivity of SnO_2 thick film sensors [7]. It was found that as the crystallite size was reduced, the sensitivity to H_2 gas enhanced at temperatures lower than 300°C, but at those higher than 350°C, the sensitivity degraded.

3.3. Electrical properties

The data on electrical conductance as a function of the reciprocal temperature of both as deposited and Palladium (Pd) sensitised films are presented in Fig. 4(a) and (b). The results of the thermal cycling experiments are also included in the same figure. The data from thermal cycling experiments conducted for four consecutive days indicate that the conductance of the as deposited film was difficult to stabilise.

Sensitisation with palladium through a novel, wet chemical technique [19–22] had helped in partial stabilisation of film conductance at high temperature (400–500 K). However, the data indicate that further experimentation is necessary for complete stabilisation of the sensor conductance. For the conductance to stabilise an equilibrium must be created between the rates of oxygen chemisorption and desorption accompanied by the transfer of electrons between adsorbed oxygen and the surface of the SnO_2 film:

$$O_2 + e^- = O_2^- \tag{5}$$

where O_2 is gaseous oxygen and O_2^- is chemisorbed oxygen acting as an electron acceptor. From the viewpoint of sensor fabrication on a commercial scale, the stabilisation of sensor conductance is important because, that ensures a stable zero level for the consideration of device design.

Utilising Eq. (1) the activation energy barrier (E_b) for activation of the conduction process was computed to be $E_b = 0.12\ (\pm)\ 0.03$ eV for 300–500 K temperature of the as deposited film and $E_b = 0.62\ (\pm)\ 0.15$ eV at 350–390 K and $E_b = 0.26\ (\pm)\ 0.06$ eV at 390–480 K for the Pd-sensitised film.

It may be noted that the conductance of as-deposited film was in the range 10^{-6}–$10^{-4}\ (\Omega)^{-1}$ while the same of the Pd-sensitised film was $\approx 10^{-9}$–$10^{-6}\ (\Omega)^{-1}$. The effective donor density (n_d) at room temperature (300 K) of both the as-deposited and the Pd-sensitised film were calculated from:

$$\sigma = n_d e \mu \tag{6}$$

where σ is electrical conductivity (calculated from measured conductance) in Ωcm^{-1}, e is the charge of an electron (1.6×10^{-19} Coulomb) and μ is the mobility. The mobility (μ) data (2–20 $cm^2\ V^{-1}\ s^{-1}$) was taken from [9] and was assumed to be constant, independent of temperature. Utilising Eq. (6) the effective donor density (n_d) was computed out to be in the range 10^{13}–10^{14} cm^{-3} for the as-deposited film and n_d was 10^{11}–10^{12} cm^{-3} for the Pd-sensitised film. Thus, the effective donor density of the Pd-sensitised film was about two orders of magnitude lower than that of the as deposited film.

The scattering mechanisms in the process of electron conduction are far from well understood, particularly in the case of tin dioxide. A partial survey of literature (Table 1) indicates that several researchers have explained their results on the basis of a variety of scattering processes and donor defect types (1, 4, 7–9, 18, 24–33). Therefore, the entire process of conduction mechanism is subsequently treated below in terms of plausible effective donor concentration and donor ionisation energy levels of the present SnO_2 films.

3.3.1. Effective donor concentration and donor ionization energy levels

The very low effective donor density in the as deposited SnO_2 films indicate the presence of a large density

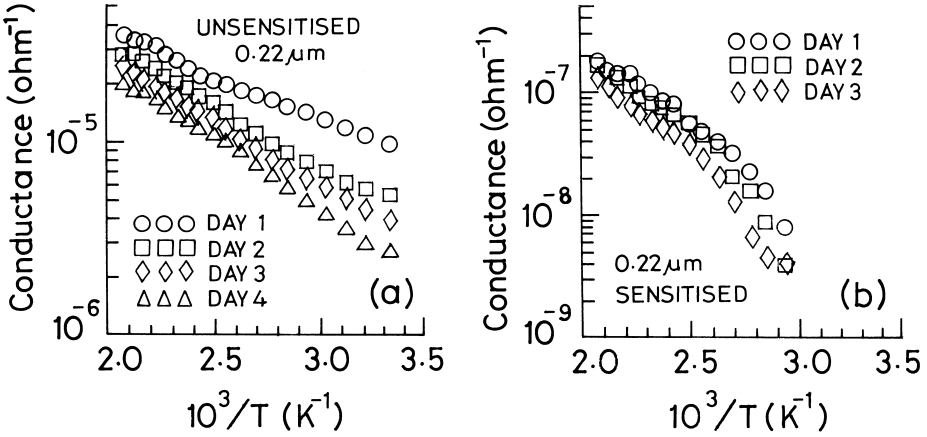

Fig. 4. Electrical conductance vs reciprocal of absolute temperature of SnO_2 thin films in (a) as-deposited and (b) Pd-sensitised conditions. Data on thermal cycling experiments for both as-deposited and Pd-sensitised films are also included.

Table 1
Literature survey on conduction mechanism in tin dioxide

Sample type	Activation energy (E_b) or Schottky barrier height in (eV)	Defect type	Year [Ref.]
TF[a]	0.01–0.04 eV	Sn interstitial	1958 [24]
Thin film	0.12 eV	Impurity band formation	1959 [25]
SC[b]	0.31–0.33 eV	No identification of donor level	1962 [26]
SC	0.21 eV (90–373 K)	Completely compensated electron trapping level	1965 [27]
	0.52 eV (90-373 K)	Shallow, unidentified donor level completely compensated	
	0.6 eV (90–373 K)	Partially compensated unidentified deep donor level	
SC	0.41–0.6 eV (573–1123 K)	0.7% Zn, no identification of donor level	1968 [28]
SC	0.3 ev (up to 1123 K)	Doubly ionized oxygen vacancy	1973 [29]
	1.0 eV ($T>$ 1123 K)	Band to band transition	
SP[c]	No value reported	Oxygen vacancy	1983 [30]
SP	1.2–1.3 eV	Schottky barrier	1987 [31]
TF	0.50–0.62 eV	Schottky barrier	1987 [31]
SP	0.28 eV (300–500 K)	Oxygen lattice vacancy	1987 [18]
	1.12 eV (750–1000 K)	Surface Schottky barrier	1987 [18]
TF (1 μm)	0.41 eV (333–380 K)	Schottky barrier	1987 [18]
	1.1 eV (800–1000 K)	Schottky barrier	1987 [18]
	0.42 eV (333–380 K) (1% CO in air)	Schottky barrier	1987 [18]
	0.5 eV (720–870 K) (1% CO in air)	Schottky barrier	1987 [18]
TF (TGS 812)	0.6–0.9 eV	Surface Schottky barrier energy	1991 [32]
Thin film	0.18 eV	Grain boundary carrier trapping	1992 [33]
TF	0.25 eV (400–740 K) 0.28 eV (Pd/SnO_2) (400–700 K)	Intrinsic donor defect level	1993 [7]
TF (0.5 mm)	0.25 ev (385–455 K)	Structural and point/planar charged defects due to dopants	1994 [9]
Thin film (30–500 nm) for $t < 70$ nm	0.05–0.08 eV (300–500 K)	*n*-Type intrinsic donor defect level	1997 [4]
SP (CoO)	0.49 eV	Surface Schottky barrier energy	1998 [1]
SP (Nb_2O_5)	1.14 eV	Surface Schottky barrier energy	1998 [1]
Thin film (0.22 μm, as-deposited)	0.12 eV (300–500 K)	Schottky barrier or modified Sn interstitial donor level	Present work
Thin film (0.22 μm, Pd-sensitised)	0.62 eV (350–390 K) 0.26 eV (390–480 K)	Doubly ionized oxygen vacancy or lowered Schottky barrier height	Present work

[a] TF, Thick film (TGS-Taguchi Sensor, Japan).
[b] SC, Single crystal.
[c] SP, Sintered pellet.

of chemisorbed species (n_t) acting as trap states for surface electrons. A large density of such trap states have always been found to reduce the effective donor concentration for thin films of ZnO and SnO_2 [7,18,20]. It is generally believed that, in the case of SnO_2 films there can be three types of mechanisms which dominates the conduction process [34]. These are: (a) for carrier concentration (n_d) less than 10^{18} cm^{-3}, charge mobility is governed by the grain boundary potential barriers; (b) for carrier concentration (n_d) greater than 10^{19} cm^{-3}, charge mobility is governed by bulk transport properties and (c) for carrier concentration (n_d) greater than 10^{18} cm^{-3} but less than 10^{19} cm^{-3}, charge mobility is governed by both the grain boundary barrier potentials and the bulk transport properties.

The present SnO_2 thin films have $n_d = 10^{13}-10^{14}\,cm^{-3}$ in the as deposited condition (see Section 3.3). Therefore, it follows from above that, the conduction mechanism in the present films is most likely to be governed by potential barrier height at the grain boundaries. For porous films of large surface to volume ratio, e.g. the present films, the depletion layer produced by the acceptor-like trap states can extend throughout the thickness (h) of the film. The conduction process through surface barrier layers in such thin films has been modeled in [18].

The basic assumptions of this model are: (a) the conduction electrons and the electrons trapped at the surface arise only from ionisation of donors and are strictly, not from the valence band; (b) within the depletion layer, the donors are fully ionised; and (c) total amount of charge in the surface states is approximately equal and opposite to the total charge on the ionised donors which resides within the depletion layer [18]. Using these assumptions and utilising the Poisson's equation of charge balance between the conduction electrons and the ionised donors, the model establishes the relationship between surface charge (Q_s) and the ionised donors (N_d) as:

$$WN_d e = Q_s \tag{7}$$

where W is the depletion width produced by surface charge (Q_s). This surface charge produces a surface potential barrier ($\Delta\phi$) across grain boundaries. This is given by [18]:

$$\Delta\phi = (Q_s)^2/(2\varepsilon\varepsilon_0 e N_d) \tag{8}$$

where, $\varepsilon\varepsilon_0$ is the dielectric constant of SnO_2.

Equating the experimentally found activation barrier value (E_b) of 0.12 eV of the as deposited tin dioxide film, to the barrier height ($\Delta\phi$) produced by the trap states, and assuming $N_d = 10^{19}\,cm^{-3}$, $\varepsilon\varepsilon_o = 2\times 10^{12}\,F\,cm^{-1}$ and $e = 1.6\times 10^{-19}$ C [18], the value of surface charge (Q_s) comes out to be of the order of 10^{-6} cm^{-2} from Eq. (8). Utilising this value of Q_{sx}, the value of depletion layer width (W) is computed to be 0.31 μm, using the Eq. (7). It may be mentioned in this connection, that a donor level (E_d) at 0.01–0.04 eV below the conduction band is generally associated with interstitial tin atom acting as donor state [24]. Therefore, the observed activation barrier value can also be associated with this donor level modified due to large density of trap states. In this case the value of $\Delta\phi$ comes out to be 0.08–0.11 eV, i.e. $(E_b - E_d)$, leading to a value of $W = 0.24\,\mu m$. This value is quite consistent with the experimentally measured value of film thickness (0.22 μm). Thus, it appears that the whole thickness of the film is essentially depleted of donor electrons; giving a very high resistive film which is also consistent with the present experimental data for the as-deposited film ie. conductance of 10^{-6}–10^{-4} $(\Omega)^{-1}$ only (see Section 3.3).

The decrease of effective donor density due to palladium surface sensitization has been associated with increased density of acceptor like chemisorbed species on ZnO films [20,35]. Usually, Pd is always found to be in the oxide state (PdO) on the surfaces of ZnO or SnO_2 [17,18,20]. The appearence of activation barrier values of 0.6 and 0.26 eV for the present Pd-sensitised SnO_2 films [Fig. 4(b)], could be associated with surface Schottky barrier energy and doubly ionised oxygen vacancy, respectively (Table 1, Refs. [28,30,31]). The high value of barrier height compared to the as deposited case may be associated with enhanced density of chemisorbed states which has the cumulative effect of lowering the effective donor density [by two orders compared to the as deposited case, Fig. 4(a and b)] as well as increasing the barrier height for conducion process. The density of chemisorbed species is extremely high in the case of Pd-sensitised SnO_2 films and hence, the donor level is pulled downward with respect to the conduction band. Similar effect was found also for ZnO thin film gas sensors fabricated by chemical deposition technique [22].

The reason for the experimentally observed activation barrier value of 0.26 eV in the high temperature (390–480 K) range of the Pd-sensitised SnO_2 films, however, is not clear. This might be due to desorption of chemisorbed species at high temperatures followed by lowering of barrier height to a negligible value. Although we have associated this with doubly ionised oxygen vacancy, this might as well be due to the lowered value of barrier height. Further experiments to resolve this issue are in progress.

4. Gas sensitivity

The data on gas sensitivity of the present tin dioxide thin film sensors are shown in Fig. 5. It may be noted that even at a low operating temperature of 150°C, the sensitivity of our SnO_2 thin film sensor towards hydrogen

(H_2) was as high as 80% (Fig. 5). This minimum of operating temperature is well below the typical range of 200–400°C, reported in the lierature [5–7,30–33,36]. The reason for this could be the very low thickness and high degree of evenly distributed fine porosity in the present films. However, the maximum sensitivity of 90% occurred as the operation temperature is increased to 200°C and decreased thereafter with a further increase in operating temperature upto 300°C (Fig. 5).

The most commonly accepted mechanisms of gas sensing for SnO_2 materials are: (a) grain boundary at the neck area between grains plays a significant role in surface adsorption of gases and such gases could be individual negative oxygen adsorbates; (b) adsorption and subsequent reaction of a toxic/combustible gas on the surface of a grain can change the Fermi level of the grain itself and the Fermi level finally determines the grain boundary potential barrier which dominates the conduction mehanism in the presence of a toxic/combustible gas; and (c) the conduction mechanism in SnO_2 thin film sensors are directly linked to change in the electronic potential barrier developed at the grain boundary when oxygen adsorbates and a toxic/combustible gas react on the surface [7,9–10,17–18,19,30,34–36]. Based on these, we propose the following qualitative model to explain the mechanism of gas sensing for the present tin dioxide thin films.

O_2^- is the most reactive surface adsorbed species on the surface of present films as mentioned earlier [Section 3.3, Eq. (5), Fig. 6(a)]. The activation by Pd may help to form a complex [19] that can incorporate hydrogen in the nascent form as [Fig. 6(b) and (c)]:

$$H_2 + Pd^{2+} = 2H(Pd^{2+}) \quad (9)$$

This nascent hydrogen is highly reactive and hence, can readily oxidize as per the following reaction [Fig. 6(d)]:

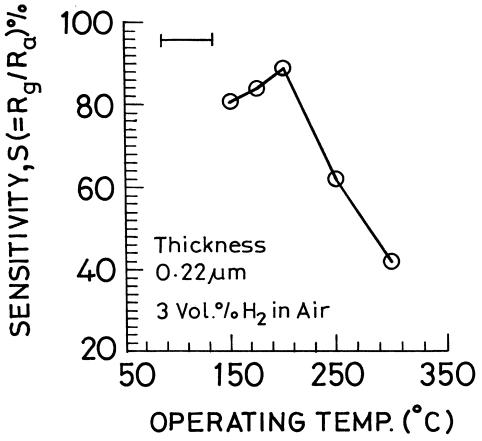

Fig. 5. Sensitivity of SnO_2 thin film as a function of operating temperature for a target of 3 vol% hydrogen with nitrogen as the carrier gas.

$$2H(Pd^{2+}) + O_2^- = 2H_2O + e^- \quad (10)$$

The extra electrons released in this process enhance the surface conductance of the thin films (Fig. 5).

The model proposed above, explains the gas sensing mechanism of the present thin film sensors qualitatively. But it does not explain the increase in gas sensitivity with rise in operating temperature. In this connection, the microstructure, particularly the size and distribution of surface porosity may also have a significant role. This is so because the surface pores may provide suitable chemisorption sites, and hence can influence the extent as well as the kinetics of the oxidation reaction (Eq. 10) between the sensor surface and the surrounding gas ambient. The minimum operating temperature found in the present work is only 150°C. At such a low temperature, the reaction region is mostly limited to the sensor surface (Fig. 6) or at the most up to the gas–solid interface. Therefore, it is suggested that the porous microstructure with nearly uniform distribution of very fine pore size [Fig. 3(a)] and the reasonably thin cross-section (0.22 μm) of the present sensors might have exerted two special influences on the proposed oxidation reaction. These are: (a) a faster rate of reaction; and (b) a reasonably higher

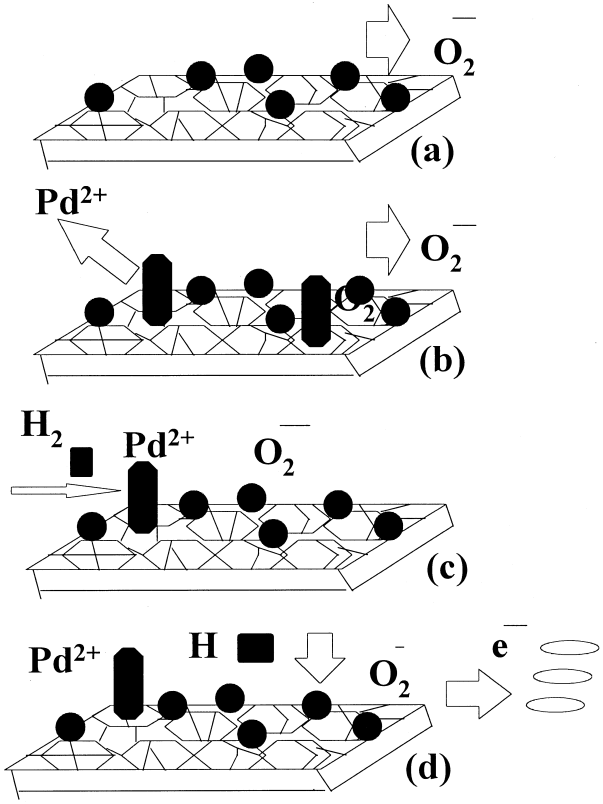

Fig. 6. Qualitative model of sensing mechanism for the present SnO_2 thin film sensors: (a) as deposited film with O_2^- adsorbates as chemisorbed species (b) palladium sensitisation causes catalytic activity; (c) reaction occurs between palladium and molecular hydrogen; and (d) catalytic oxidation reaction [Eq. (10)] between surface chemisorbed species and hydrogen yields conduction electrons.

degree of completeness of the reaction. These would cause high sensitivity at such low operating temperature as has been observed in the present work (Fig. 5).

It may be noted further from the data presented in Fig. 5, that the gas sensitivity also increased with operating temperature; reached maximum (90%) at 200°C and decreased thereafter with farther enhancement in the operating temperature. This temperature dependency can be rationalised in terms of two particular aspects: (a) depending upon the operating temperature, the chemical nature of the surface adsorbed species may change and (b) the reaction mechanism of a given toxic/combustible gas with the chemisorbed species may change due to the change in operating temperature [6–11,17–22,30–32,34–36]. Based on these considerations, the following picture of temperature dependency can be developed.

As the operating temperature increases, the catalytic oxidation rate process [Eq. (10)] on the surface of the present SnO_2 thin films becomes thermally activated and hence, faster. As a result, the number of conduction electrons released per unit time at higher operating temperature would be more than the number of conduction electrons released per unit time at lower operating temperatures. This should enhance the conductivity of the film. As a consequence the film resistivity drops and hence, the gas sensitivity [Eq. (2)] enhances initially in the presence of hydrogen when the operating temperature is enhanced (Fig. 5).

However, the continuity of this process is also dependent on the availability of the chemisorbed species on the sensor surface. As the operating temperature is enhanced, the balance between the rate of adsorption and desorption of chemical species on the surface becomes important. This is so because the surface oxygen adsorbates and hydrogen react to release electrons as well as H_2O [Eq. (10), Fig. 6]. At higher operating temperatures this H_2O would be desorbed to leave an empty adsorption site on the surface of SnO_2 thin film [2–8,10,17–19,32–34,36]. It is at such sites that atmospheric oxygen would again be re-adsorbed to act subsequently as chemisorbed species; which would again react with hydrogen to continue the process of gas sensing. Thus, at temperatures higher than the cut-off temperature (200°C for the present thin film sensors), the rate of H_2O desorption per unit time may sufficiently exceed the rate of re-adsorption of oxygen per unit time, thereby leading to a net decrease in the number of chemisorbed species available per unit time on the sensor surface. This lack in number of chemisorbed species availbale per unit time on the sensor surface can slow down the time rate of catalytic oxidation reaction; leading to a decrease in net yield of conduction electrons. If that is the scenario, the gas sensitivity should decrease with operating temperatures above the cut-off temperature. This proposed rationale is consistent with the present experimental observations (Fig. 5). However, further studies are necessary to provide detailed verifications of these suggestions.

5. Conclusions

The major conclusions of the present work are as follows:

(a) Tin dioxide thin film sensors were fabricated by a modified chemical deposition technique. The process involved successive dipping of a commercial glass substrate in a sodium sulphide (Na_2S) bath (0.025 M) kept at room temperature and a stannous chloride ($SnCl_2$) bath (0.025 M) kept at 85°C. This sequence was repeated for the requisite number of times to induce growth of tin sulphide (SnS) film. Finally, the SnS film was oxidised for 1 h at 400°C in air to obtain the porous, thin films of SnO_2.

(b) Up to 50 dips, the deposition process was fairly linear, with a rate of 0.28 μm/dip/mol. At a higher number of dips ($N = 50-300$), the growth of film thickness followed a distinctly non-linear trend. $SnCl_2$ bath temperatures below 85°C do not seem to have any significant influence on film thickness. At temperatures greater than 85°C, film thickness increased slightly with bath temperature. Further, the film thickness also increased non-linearly with enhancement in $SnCl_2$ bath concentration. The data, however, show two different slopes at concentrations less than 0.1 M and greater than 0.1 M. Up to 50 dips, the phase purity of the present SnO_2 films is preserved. But, as the films grew thicker e.g. $N = 100$, the Sn_2O_3 phase appeared along with the SnO_2 phase. SEM photographs indicate that these films had very fine crystallite size in the range of a few tens to a few hundreds of angstroms (Å) only and a porous microstructure with very fine pores distributed nearly uniformly on the film surface.

(c) From the experimental data on 0.22 μm thin films of SnO_2, the activation energy barrier (E_b) for activation of the conduction process in air was computed out to be $E_b = 0.12 (\pm) 0.03$ eV for 300–500 K temperature of the as deposited film and $E_b = 0.62 (\pm) 0.15$ eV at 350–390 K and $E_b = 0.26 (\pm) 0.06$ eV at 390–480 K for the Pd-sensitised film.

(d) The gas sensitivity of the palladium sensitised tin dioxide thin fim sensors was evaluated in air inside a closed quartz tube furnace as a function of the operating temperature (150–300°C) for a fixed concentration (3 vol%) of hydrogen gas with nitrogen as the carrier gas. The response of the palladium sensitised tin dioxide thin film sensors could be recorded at an operating temperature of as low as 150°C. Maximum sensitivity of 90% occurred at a

low temperature of only 200°C. Above this cut-off temperarure, sensitivity suffered moderate degradation.

Acknowledgements

The authors gratefully acknowledge the experimental assistance of Dr. Mrs. S. Sen, Dr. A. K. Chakraborty, Mr. Jalaluddin Mandal and Mr. N. Bharati. One of us (P.M.) is also thankful to the Director, Central Glass and Ceramic Research Institute, Calcutta 700 032, India for the provision of financial assistance in the form of a Reseach Fellowship.

References

[1] S.P. Pianaro, R. Beuno, P. Olivi, E. Longo, J.A. Varela, J. Mater. Sci. Materials in Electronics 9 (1998) 159.
[2] F. Cerilli, S. Kaciulis, G. Mattogno, A. Galdiks, A. Mironas, B. Schknis, A. Schknis, Thin Solid Films 315 (1998) 310.
[3] C.H. Lin, L. Zhang, Y.-J. He, Thin Solid Films 304 (1997) 13.
[4] A.I. Evashchenko, I.A.I. Karner, G.A. Kiosse, I.Yu. Maroncluk, Thin Solid Films 303 (1997) 292.
[5] C. Xu, J. Tamai, N. Yamazoem, Sensors and Actuators B3 (1991) 147.
[6] V.V. Malyshev, A.A. Valiliev, A.V. Eryshkin, E.A. Koltypil, Y.I. Buturlil, A.I. Buturlil, V.A. Zikin, G.B. Chakhunashvil, Sensors and Actuators B10 (1992) 11.
[7] K.H. Song, S.J. Park, J. Mater. Sci. Materials in Electronics 4 (1993) 249.
[8] D.D. Lee, D.H. Choi, Sensors and Actuators B1 (1990) 231.
[9] A. Massed, J. Brunex, H. Cachet, M. Forment, J. Mater. Sci. 29 (1994) 5095.
[10] K.D. Schierbaum, J. Geiger, U. Weimar, W. Gopel, Sensors and Actuators B13 (1993) 143.
[11] K. Nomura, H. Shiozawa, T. Takada, H. Reuther, E. Richter, J. Mater. Sci. Materials in Electronics 8 (1997) 301.
[12] D. Liu, Q. Bang, H.L.M. Ling, H. Chem, J. Mater. Res. 10 (1995) 1516.
[13] Y. Inoue, J. Matsuo, J. Kato, J. Chem. Soc. Faraday Trans. 86 (1990) 2611.
[14] S.S. Park, J.D. Mackanjie, Thin Solid Films 258 (1995) 268.
[15] M. Kanamari, Y. Okamato, Y. Ohya, Y. Takahashi, J. Ceram. Soc. Japan 103 (1995) 113.
[16] G.S. Trivikrama Rao, S.S. Madhavendra, J. Mater. Sci. Lett. 14 (1995) 529.
[17] G. Heiland, D. Kohl, in: T. Seiyama (Ed.), Chemical Sensor Technolgy, vol. 1, Elsevier, Oxford, 1988, p. 15.
[18] J.F. McAleer, P.J. Moseley, J.O.W. Morris, D.E. Williams, J. Chem. Soc. Faraday Trans. 83 (1987) 1323.
[19] A.K. Mukhopadhyay, P. Mitra, A.P. Chatterjee, H.S. Maiti, J. Mater. Sci. Lett. 17 (1998) 625.
[20] P. Mitra, A.P. Chatterjee, H.S. Maiti, Mater. Lett. 35 (1998) 33.
[21] A.K. Mukhopadhyay, P. Mitra, D. Chattopadhyay, H.S. Maiti, J. Mater. Sci. Lett. 15 (1996) 431.
[22] P. Mitra, A.P. Chatterjee, H.S. Maiti. J. Mater. Sci. Materials in Electronics (in press).
[23] G. Pfaff, J.P. Bonnet, Ceram. Int. 23 (1997) 257.
[24] K. Ishiguro, T. Sasaki, T. Arai, I. Imai, J. Phys. Soc. Japan 13 (1958) 1296.
[25] V.K. Miloslavskii, Opt. Spectrosc. 7 (1959) 154.
[26] E.E. Kohnke, J. Phys. Chem. Solids 23 (1962) 1557.
[27] J.E. Houston, E.E. Kohnke, J. Appl. Phys. 36 (1965) 3931.
[28] H.E. Mathews, E.E. Kohnke, J. Phys. Chem. Solids 29 (1968) 653.
[29] S. Samson, C.G. Fonstad, J. Appl. Phys. 44 (1973) 4618.
[30] M.K. Paria, H.S. Maiti, J. Mater. Sci. 18 (1983) 2101.
[31] V. Lantto, P. Rolppainen, L. Leppavuori, Sensors and Actuators B14 (1987) 149.
[32] F.G. Schmitte, G. Wiegleb, Sensors and Actuators B4 (1991) 473.
[33] V. Demarne, A. Grisel, R. Sanjines, D. Rosenfield, F. Levy, Sensors and Actuators B7 (1992) 704.
[34] H.L. Hartnagel, A.L. Dawar, A.K. Jain, C. Jagadish, Semiconducting Transparent Thin Films, Institute of Physics, Bristol, UK, 1995, pp. 134–217.
[35] M. Katsura, M. Shiratori, T. Takahasi, Y. Yokomizo, N. Ichinose, in: T. Seiyama (Ed.), Chemical Sensors. Kodansha, Tokyo, 1983, p. 101.
[36] K.D. Schierbaum, J. Geiger, U. Weimar, W. Gopel, Sensors and Actuators B7 (1992) 709.